CONF-830874--23

UCRL- 89756
PREPRINT
UCRL--89756

DE83 017473

PRECISION SUPPORT OF ANNULAR OPTICS

J. W. Roblee
D. W. Stillman
S. R. Patterson

This paper was prepared for submittal to
SPIE's 27th Annual International
Technical Symposium and Instrument Display,
San Diego, CA, August 21-26, 1983

August 1983

Lawrence Livermore National Laboratory

DISCLAIMER

DISCLAIMER

PRECISION SUPPORT OF ANNULAR OPTICS

By

J. W. Roblee
D. W. Stillman
S. R. Patterson

Lawrence Livermore National Laboratory
P. O. Box 808, L-792, Livermore, California 94550

Abstract

A quantitative description of the deformation of an annular optical element subject to external forces has been developed. Expressions applicable when the width of the element is small compared to its radius provide distortion data for both free rings and rings supported on thin-wall cylinder segments ('tangent flanges'). This data may be used to guide the design of fixtures for diamond turning large annular optics.

Introduction

Recent interest in annular laser resonators has focused attention on the problem of manufacturing and mounting ring-shaped optical elements. Of particular concern is the ability to maintain a very high degree of azimuthal symmetry in the optic. This paper presents an analytic approach to the calculation of azimuthal elastic deformation of a ring, and of a ring supported by a cylindrical shell ('tangent flange'). In all cases, the optic and its support are considered to be azimuthally symmetric and constructed of an isotropic elastic material. Solutions are presented for the general loading case. A right-hand coordinate system and right-hand rule for moment definition are used throughout the following discussion. Table 1 lists the notation used in the equations which follow. The derivations[4] leading to the results presented here are lengthy and therefore not included in this paper.

Ring Element

The ring element is modelled using the basic approximations of curved beam theory. That is, the cross-section is assumed to remain undistorted during bending, plane sections remain plane, and deformation due to bending dominates deformation due to shear and ring extension. It is easily seen that these approximations are valid if the characteristic radial dimension of the ring cross-section is small compared to the ring radius. Under these assumptions, the elastic properties of the ring are completely determined by the material modulus and the four section moments of inertia, (C_w is a torsion warping factor),

$$\begin{aligned} I_r &= \int r^2 \, dr \, dz \\ I_z &= \int z^2 \, dr \, dz \\ I_{rz} &= \int r \, z \, dr \, dz \\ J &= C_w \int (r^2 + z^2) \, dr \, dz \end{aligned}$$

The ring loading has six degrees of freedom: three each of applied force and moment. It is shown in plate and shell theory[1,2], however, that the effects of distributed moment loading about the r- and z-axes may be approximated by replacing them with a statically equivalent set of forces added to the remaining four:

$$F_z^{new} = F_z^{old} + \frac{1}{a}\frac{d}{d\theta} M_{rz}$$

$$F_\theta^{new} = F_\theta^{old} + \frac{1}{a}\frac{d}{d\theta} M_{z\theta}$$

$$F_r^{new} = F_r^{old} + \frac{1}{a} M_{z\theta}$$

A general, non-symmetric loading case may be considered by resolving the load and resulting deformation into their Fourier components. Since the problem involves linear elasticity, each component may be considered separately, and the results combined after calculation. The theory presented here provides the four dimensional compliance matrix connecting the n^{th} Fourier component of the three distributed force loadings and moment loading about the azimuthal direction to the resulting three directional displacements and rotation about the azimuthal direction, where the the loading is taken on the shear center of the ring cross-section (u and f_0 are 90° out of phase with the other components),

$$\vec{x} = \begin{Bmatrix} u \\ v \\ w \\ \phi \end{Bmatrix} \qquad \vec{f} \equiv \begin{Bmatrix} f_\theta \\ f_z \\ f_r \\ m_z \end{Bmatrix} \qquad \vec{x} = C \, \vec{f}$$

mlg

The compliance matrix is determined by assuming an isotropic elastic constitutive relation between stress and strain, and the appropriate equilibrium equations of curved beam theory.[3] The solution of the resulting equations yields the following value of compliance:

$$\text{for } n>1 \qquad C = \frac{a^3}{(n^2-1)^2 E\Delta}\begin{bmatrix} \frac{I_r}{n^2} & \frac{I_{rz}}{n} & \frac{-I_r}{n} & \frac{-I_{rz}}{an} \\ \frac{I_{rz}}{n} & (I_z + \frac{2(1+\nu)\Delta}{n^2 J}) & -I_{rz} & -\frac{1}{a}(I_z + \frac{2(1+\nu)\Delta}{J}) \\ \frac{-I_r}{n} & -I_{rz} & I_r & \frac{I_{rz}}{a} \\ \frac{-I_{rz}}{an} & \frac{-1}{a}(I_z + \frac{2(1+\nu)\Delta}{J}) & \frac{I_{rz}}{a} & \frac{1}{a^2}(I_z + \frac{2n^2(1+\nu)\Lambda}{J}) \end{bmatrix}$$

This compliance matrix is symmetric, as demanded by the Maxwell-Betti reciprocity theorem. Also, the compliance matrix scales with the Young's modulus. If one of the principal axes of the ring cross-section is in the plane of the ring, then I_{rz} is zero and many of the off-diagonal cross coupling terms go to zero. When this is not the case, radial forces lead to axial displacement. The compliance matrix also displays a strong dependence on the Fourier index, n. This dependence on n suggests that only the first several terms in the expansion will be necessary for a reasonably accurate solution to most loading problems.

One may make a first order correction for the effect of ring extension and shear, by using the stress distribution resulting from the bending solution. The result is a shear compliance which is added to the compliance matrix described above;

$$C^{shear} = \frac{a}{En^2}\begin{bmatrix} \frac{1}{A} + \frac{2(1+\nu)}{A_{sr}(n^2-1)} & 0 & -\frac{2(1+\nu)n}{A_{sr}(n^2-1)} & 0 \\ 0 & \frac{2(1+\nu)}{A_{sz}} & 0 & 0 \\ \frac{-2(1+\nu)n}{A_{sr}(n^2-1)} & 0 & \frac{2(1+\nu)n^2}{A_{sr}(n^2-1)} & 0 \\ 0 & 0 & 0 & 0 \end{bmatrix}$$

Note that symmetry is still maintained. If the shear contribution is compared to that from bending, one notes a much weaker dependence on the radius and the mode number. In addition, for typical ring cross-sections, the shear areas are smaller than the principal moments of inertia. Therefore, for small n and large a, the terms in the shear compliance matrix are much smaller than the contributions from bending.

The ring depicted in Figure 1 has been used for test calculation. Its thickness to radius ratio of 1:4 is pushing the limits of thin ring theory. The standard criteria for an accurate solution is a ratio less than 1:10. For comparison purposes, the deformation of the cross-section has also been calculated with a finite element code, GEMINI. Some of the resulting compliances, using a modulus of 3×10^7 PSI and a Poisson ratio of .3, are shown in Figure 2. The finite element compliance has been calculated with several mesh spacings, to assure mesh-independence and the displacements are calculated from a best fit line through the deformed optical surface of the ring. All the displacements quoted in the figures are of the midpoint of the optical surface. The disagreement at large index is the result of cross-section distortion appearing in the finite-element model as a substantial part of the total deformation. Figure 3 shows the relative magnitudes of flat surface displacement and out-of-flat deformation. It is important to note that the total contribution from these Fourier modes is small, so the differences are not of significance for typical loading cases.

The solution can be generalized to incorporate a load center offset from the ring shear center by deriving transformation matrices for the displacement and force vectors. These transformation matrices can then be combined with the compliance matrix to define a new, effective compliance matrix. If T_x is the displacement transformation and T_f is the force transformation, then the new compliance matrix is found by transforming force to the shear axis and using the inverse transform to return displacement to the drive point:

$$C^{new} = T_x^{-1} C^{old} T_f$$

$$T_x^{-1} = \begin{bmatrix} 1 & \frac{-ne_z}{a} & \frac{-ne_r}{a} & 0 \\ 0 & 1 & 0 & e_r \\ 0 & 0 & 1 & -e_z \\ 0 & 0 & 0 & 1 \end{bmatrix} \qquad T_f = \begin{bmatrix} 1 & 0 & 0 & 0 \\ \frac{-ne_z}{a} & 1 & 0 & 1 \\ \frac{-ne_r}{a} & 0 & 1 & 0 \\ 0 & e_r & -e_z & 1 \end{bmatrix}$$

Cylindrical Shell Element

The cylindrical shell support is described by force and displacement vectors at each end. The compliance, then, is an 8x8 matrix relating pairs of force vectors to pairs of displacement vectors. An analytic solution for the compliance matrix may be found in the thin shell approximation[4] (thickness much less than radius and length). The nature of the solution depends on the eight complex roots of the characteristic equation of the system, k_{1-8}:

$$(1+4g^2)k^8 - 4(1+g^2)n^2k^6 + ((6+g^2(1-\nu^2))n^4 - (8-2\nu^2)n^2 + (1-\nu^2)(\frac{1}{g^2} + 4))k^4 - 4n^2(n^2-1)^2k^2 + n^4(n^2-1)^2 = 0$$

where, $$g^2 = \frac{t^2}{12a^2}$$

Typically, these roots may be grouped into two sets of four, one describing membrane behavior, and the other describing bending effects. To implement the following description of the solution, it is convenient to set k_{1-4} equal to the small roots, and k_{5-8} equal to the large roots. We may then express the compliance matrix with the help of several intermediate quantities as described below. The index i runs from one to eight, and P_u, P_v, and P_w are solutions to the matrix equation,

$$\begin{bmatrix} \frac{(1+\nu)}{2}nk_i & k_i^2 - \frac{(1-\nu)}{2}n^2 & \nu k_i \\ (1+g^2)n^2 + \frac{(1-\nu)}{2}(1+4g^2)k_i^2 & \frac{(1+\nu)}{2}nk_i & n(1+g^2(n^2-(2-\nu)k_i^2)) \\ n(1+g^2(n^2-(2-\nu)k_i^2)) & \nu k_i & 1+g^2(n^2-k_i^2)^2 \end{bmatrix} \begin{Bmatrix} P_{ui} \\ P_{vi} \\ P_{wi} \end{Bmatrix} = 0$$

Eight non-trivial solutions of this relation are assured because the left side of the characteristic equation satisfied by the k_i is just the determinant of the above matrix. One may then produce the compliance matrix, C, as follows:

$$Q_{N\Theta i} = \frac{D(1-\nu)}{2a}((1+4g^2)k_iP_{ui} - nP_{vi} + 4g^2nk_iP_{wi})$$

$$Q_{NZi} = \frac{D}{a}(\nu nP_{ui} + k_iP_{vi} + \nu P_{wi})$$

Where $D = \frac{Et}{(1-\nu^2)}$

$$Q_{QZi} = \frac{Dg^2}{a}(-(2-\nu)nk_iP_{ui} + k_i(k_i^2 - n^2(2-\nu))P_{wi})$$

$$Q_{MZi} = -Dg^2(\nu nP_{ui} + (\nu n^2 - k_i^2)P_{wi})$$

4x8 matrices,

$$\hat{P} = \begin{bmatrix} \cdot & \cdot & \cdot & P_{ui} & \cdot & \cdot & \cdot & \cdot \\ \cdot & \cdot & \cdot & P_{vi} & \cdot & \cdot & \cdot & \cdot \\ \cdot & \cdot & \cdot & P_{wi} & \cdot & \cdot & \cdot & \cdot \\ \cdot & \cdot & \cdot & a^{-1} k_i P_{wi} & \cdot & \cdot & \cdot & \cdot \end{bmatrix} \qquad \hat{Q} = a \begin{bmatrix} \cdot & \cdot & \cdot & -Q_{N\Theta i} & \cdot & \cdot & \cdot & \cdot \\ \cdot & \cdot & \cdot & -Q_{NZi} & \cdot & \cdot & \cdot & \cdot \\ \cdot & \cdot & \cdot & Q_{QZi} & \cdot & \cdot & \cdot & \cdot \\ \cdot & \cdot & \cdot & -Q_{MZi} & \cdot & \cdot & \cdot & \cdot \end{bmatrix}$$

8x8 matrices,

$$S = \begin{bmatrix} \exp(k_1 L/a) & & & & \\ & \ddots & & \text{--0--} & \\ & & \exp(k_i L/a) & & \\ & \text{--0--} & & \ddots & \\ & & & & \exp(k_8 L/a) \end{bmatrix} \qquad P = \begin{bmatrix} \hat{P} \\ \hline \hat{P}\, S \end{bmatrix} \qquad Q = \begin{bmatrix} \hat{Q} \\ \hline -\hat{Q}\, S \end{bmatrix}$$

$$C = P\, Q^{-1}$$

It is clear from the form of C that the initial normalization of P_{ui}, P_{vi}, and P_{wi} do not affect the result. C is also real and symmetric, notwithstanding the complex elements of P, Q, and S. A general 8x8 matrix inversion need not be performed to calculate the inverse of Q, since we may take advantage of prior knowledge of the block form of Q and the symmetry of C. In general, the computation of C is a straightforward task that may be accomplished in much less time than the comparable finite element calculation.

Combining Elements

The static response of a structure consisting of a cylindrical shell with rings attached at either end may be readily calculated by considering the inverse of the compliance matrix, the stiffness matrix K. Using the block form for K and denoting the rings attached to the shell by R1 and R2, one may write;

$$K = \begin{bmatrix} K^{R1} & \vdots & 0 \\ \hline 0 & \vdots & K^{R2} \end{bmatrix} + K^{shell} = \begin{bmatrix} K_{11} & \vdots & K_{12} \\ \hline K_{21} & \vdots & K_{22} \end{bmatrix}$$

Once the stiffness has been determined, specific boundry conditions may be introduced to determine response characteristics of the structure. Of particular interest is the case in which one end of the structure (the optical surface) is free. In this case, one may reduce the structure to an equivalent ring and a displacement transfer function by solving the equation set,

$$\vec{f}_1 = K_{11}\, \vec{x}_1 + K_{12}\, \vec{x}_2 \qquad \vec{f}_2 = 0 = K_{21}\, \vec{x}_1 + K_{22}\, \vec{x}_2$$

yielding,

$$\vec{f}_1 = (K_{11} - K_{12}\, K_{22}^{-1}\, K_{21})\, \vec{x}_1 = K^{equiv}\, \vec{x}_1 \qquad \vec{x}_2 = -K_{22}^{-1}\, K_{21}\, \vec{x}_1$$

This procedure may be repeated indefinitely to reduce a serially-connected system of ring/shell elements to a single equivalent ring and displacement transfer function. In executing such a reduction, it is not necessary to deal with matrices of order greater than four, thus suiting the algorithm for implementation on smaller computers than are typically used for finite element analysis.

As an example of the procedure, the transfer function has been calculated for the ring of Figure 1 supported on a cylindrical shell of radius 22.5 inches, length 3 inches and thickness 0.1 inch. The connection between the two elements is taken as the intersection of the cylindrical shell and the outside surface of the ring; the offset of this point from the shear center of the ring is accounted for in the fashion described above. The transfer function calculated gives an approximation to the influence of base tolerance on the response of an optic mounted on such a 'tangent flange' where the base is much more rigid than the flange. The results of the calculation are shown in Figure 4, along with the results of a finite element model of the same structure.

References

(1) Flügge, W., Stresses in Shells, Springer-Verlag New York Inc., 1980.

(2) Gol'denveizer, A.L., Theory of Elastic Thin Shells, Pergamon Press, 1961.

(3) Meck, H.R., "Three-Dimensional Deformation and Buckling of a Circular Ring of Arbitrary Section," Journal of Engineering for Industry, Trans. of ASME, Feb., 1969, pp. 266-272.

(4) Roblee, J.W., "Cylindrical Shell and Ring Deformation Subject to Arbitrary Edge Loading," Lawrence Livermore National Laboratory, to be published, (UCRL-).

Table 1

Notation Used for Analytical Ring and Shell Calculation

Calculations use a right-hand (R,θ,Z) cylindrical coordinate system, where the Z-axis is an axis of symmetry for the problem. Notation is generally consistent with that used by Flügge. Lower case letters used for force or displacement indicate a Fourier component.

A	Ring cross-section area
A_{sr}	Ring effective radial shear area
A_{sz}	Ring effective axial shear area
a	Radius of ring shear center or shell
C_w	Warping factor for torsion
e_r, e_z	Offset from ring shear axis to mounting point in r- and z- directions
E	Modulus of Elasticity
G	Shear modulus
I_r	Ring moment of inertia about r-axis
I_z	Ring moment of inertia about z-axis
I_{rz}	Ring product moment of inertial
J	Ring modified polar moment of inertia
k_{1-8}	Roots of the shell characteristic equation
L	Length of shell
F_r	Radial loading
F_z	Axial loading
F_θ	Tangential loading
M_z	Moment load about positive θ direction
M_{rz}	Moment load about positive r direction
$M_{z\theta}$	Moment load about negative z direction
n	Fourier mode number
t	Shell thickness
U	Tangential displacement
V	Axial displacement
W	Radial displacement
Δ	$I_r I_z - I^2_{rz}$
Φ	Rotation about θ direction
ν	Poisson's ratio

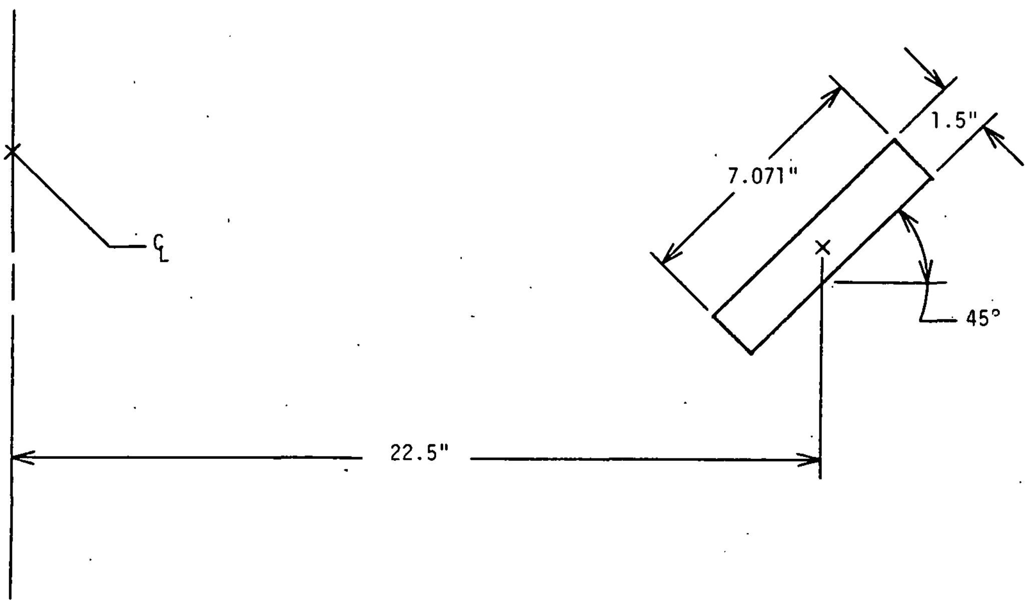

Figure 1. Test Ring Element

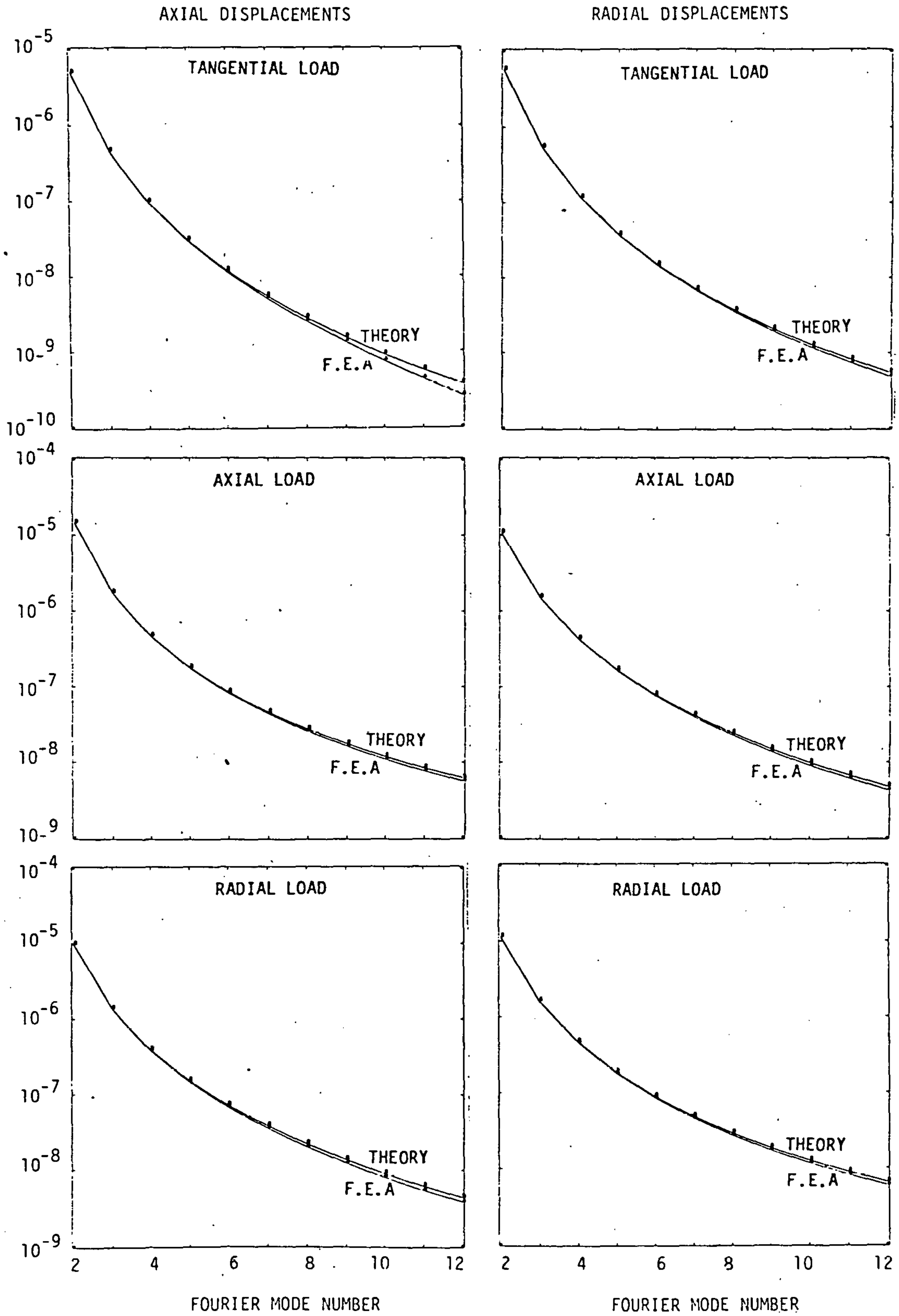

Figure 2. Comparison of Theory and Finite Element Analysis for Surface Displacements of the Free Ring Subject to Unit Centroidal Loading (in/lb).

Auspices

Work performed under the auspices of the U.S. Department of Energy by the Lawrence Livermore National Laboratory under contract number W-7405-ENG-48.

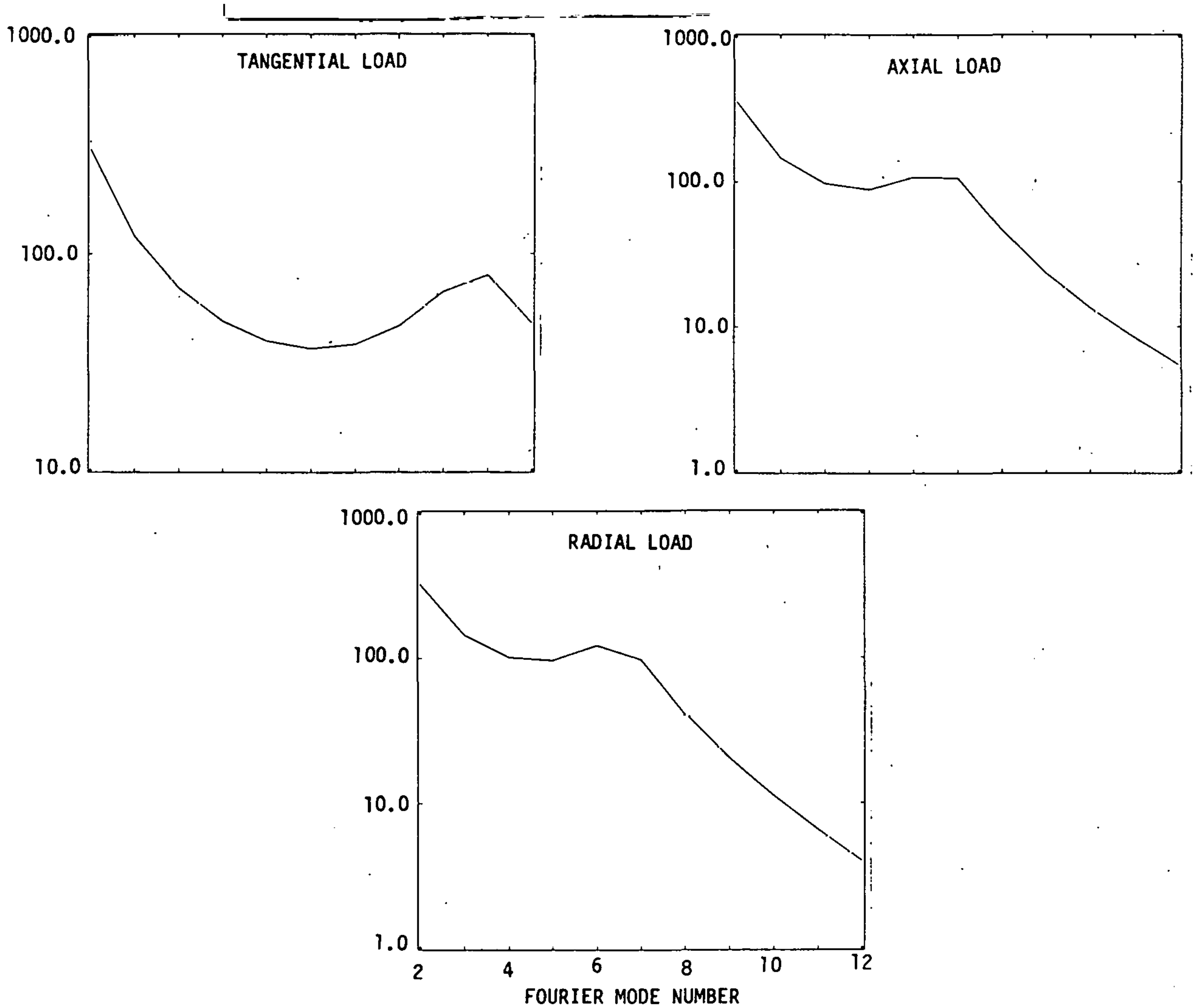

Figure 3. Ratio of Flat Surface Displacement to Out-of-Flat Deformation in the Finite Element Analysis (rms in/in).

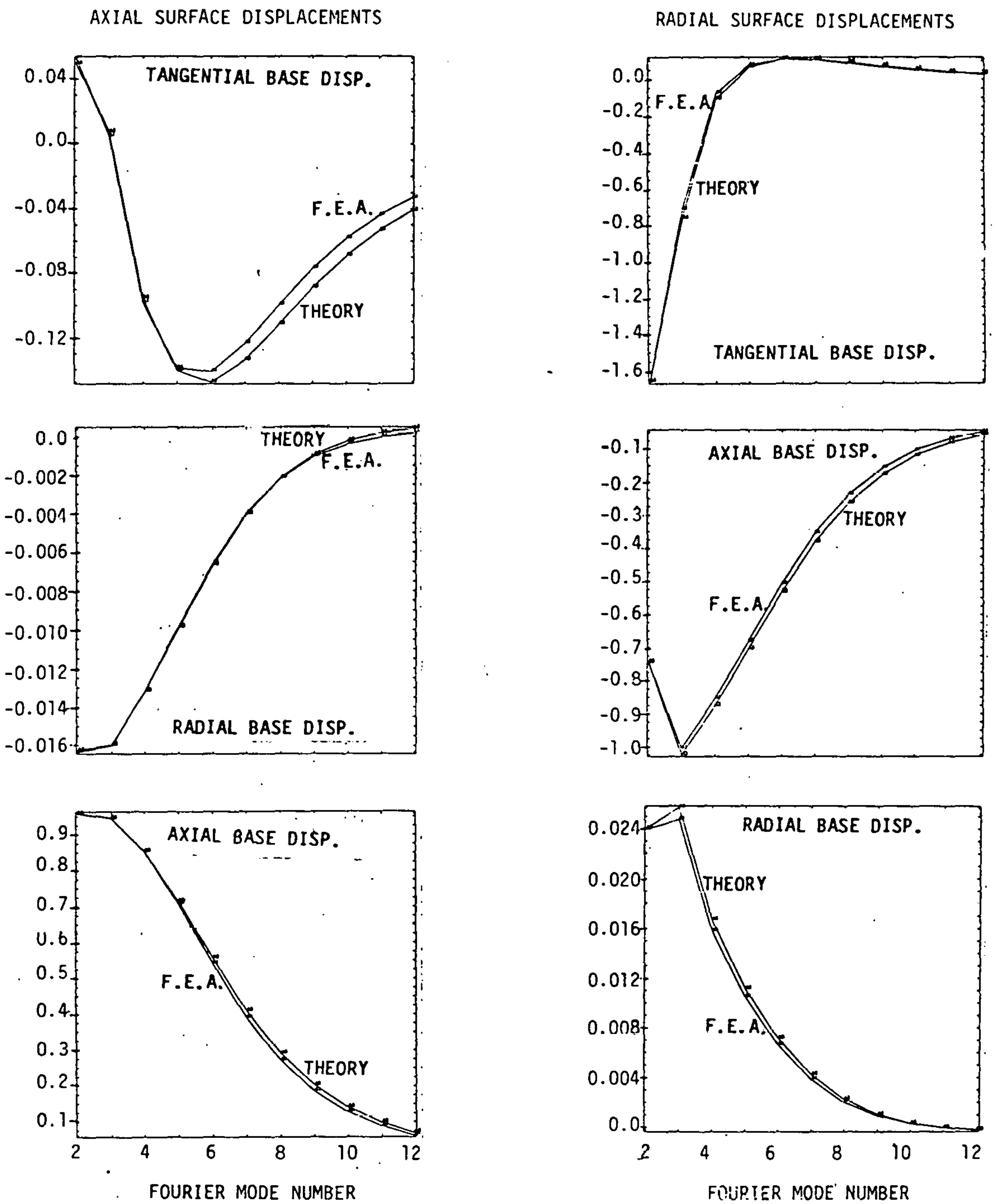

Figure 4. Comparison of Theory and Finite Element Analysis for Surface Displacements of a Ring with Tangent Mount for a Unit Displacement at the Base (in/in).

Technical Information Department · Lawrence Livermore Laboratory
University of California · Livermore, California 94550